Dissolved organic carbon retention by coprecipitation during the oxidation of ferrous iron

Dissolved organic carbon retention by coprecipitation during the oxidation of ferrous iron

Marcella Sodano[a], Cristina Lerda[a], Roberto Nisticò[c], Maria Martin[a], Giuliana Magnacca[b], Luisella Celi[a], Daniel Said-Pullicino[a,*]

[a] *Soil Biogeochemistry, Department of Agricultural, Forest and Food Sciences, University of Torino, Largo P. Braccini 2, 10095 Grugliasco, Italy*

[b] *Department of Chemistry, University of Torino, Via P. Giuria 7, 10125 Torino, Italy*

[c] *Department of Applied Science and Technology DISAT, Politecnico di Torino, C.so Duca degli Abruzzi 24, 10129 Torino, Italy*

*Corresponding Author: Daniel Said-Pullicino, Dept. of Agricultural, Forest and Food Sciences, University of Torino, Largo Paolo Braccini 2, 10095 Grugliasco, Italy. (E-mail: daniel.saidpullicino@unito.it)

Abstract

The adsorption of dissolved organic carbon (DOC) on iron (Fe) (hydr)oxides represents an important stabilization mechanism for soil organic matter (OM) and contributes to soil C accumulation. However, in soils that experience periodic fluctuations in redox conditions the interaction between DOC and Fe (hydr)oxides may not only involve organic coatings on mineral surfaces, but also Fe-DOC coprecipitates that form during the oxidation of soil solutions containing important amounts of DOC and Fe^{2+}. The aim of this work is to provide new insights into the mechanisms involved, and the amount and selectivity of C retained during the coprecipitation process. A series of Fe-OM associations with increasing C loading was synthesized at pH 6 by surface adsorption or coprecipitation (oxidation of ferrous iron) utilizing rice-straw derived dissolved organic matter. The kinetics of Fe^{2+} oxidation and complexation, and the total and selective retention of DOC during the coprecipitation process were evaluated. Moreover, synthesized associations, as well as a field coprecipitate collected *in situ* from a paddy soil, were studied by X-ray diffraction, N_2 gas adsorption-desorption isotherms, electrophoretic mobility measurements and thermogravimetric analyses. Coprecipitation resulted in higher organic C contents (49-213 mg g^{-1}) with respect to adsorbed systems (18-47 mg g^{-1}), and favoured the inclusion of OM within highly aggregated associations having particularly low BET specific surface areas. Although coprecipitation led to a strong, selective retention of aromatic constituents, the initial complexation of Fe^{2+} by aliphatic carboxylic moieties and precipitation as C-rich Fe-OM associations contributed to the total C retention, particularly at higher C/Fe ratios. These aliphatic complexes formed during coprecipitation may play an important, though often underestimated, role in C stabilization in soils experiencing frequent redox fluctuations and often characterized by elevated soluble Fe^{2+} and DOC concentrations.

Keywords: Ferrihydrite, surface adsorption, complexation, coprecipitation, paddy soils, selective retention.

1. Introduction

Sorption of dissolved organic matter (DOM) onto iron (Fe) (hydr)oxides is known to play an important role in the stabilization and accumulation of organic carbon (C) in soils (Eusterhues et al., 2005; Kaiser and Guggenberger, 2000). However, in hydromorphic soils the retention of organic C by soil minerals and its subsequent stabilization against microbial decomposition largely depends on redox state (Kögel-Knabner et al., 2010). In fact, changes in soil redox conditions can strongly influence the association between Fe (hydr)oxides and soil organic matter (OM) with important implications on C stabilization.

Paddy soils are hydromorphic soils formed under intense anthropogenic influence and generally subjected to periodically fluctuating redox conditions induced by specific agricultural management practices (flooding, puddling and drainage; Kögel-Knabner et al., 2010). These soils are known to accumulate significant amounts of OM in the topsoil (Wissing et al., 2014), however the mechanisms of OM accumulation under paddy management are not well understood. Apart from the incomplete decomposition of OM under anaerobic conditions (i.e. biological capacity; see Baldock et al., 2004), direct interactions with ubiquitous Fe (hydr)oxides (i.e. chemical protection) may contribute significantly to the long-term stabilization of OM (Wissing et al., 2013).

Reductive dissolution of Fe (hydr)oxides under anoxic conditions releases Fe^{2+} into solution which may be readily oxidized by O_2 and precipitated in the form of short-range ordered hydroxides such as ferrihydrite, when oxic conditions are rapidly re-established (Said-Pullicino et al., 2016; Schwertmann, 1991). Under these conditions, highly disordered Fe phases often form in the presence of elevated concentrations of DOM through the process of coprecipitation. In contrast to surface adsorption, coprecipitation may involve different mechanisms of Fe-OM association, namely inclusion (i.e., included within the crystal structure) and occlusion (i.e., physical entrapment within the growing crystal), as well as adsorption on neo-formed (hydr)oxides (Kleber et al., 2014 and references therein). Unlike adsorption, where DOM is mainly retained by ligand exchange at the surface of pre-existing Fe oxides, coprecipitation may result in the formation of a mixture of pure and OM-rich Fe (hydr)oxides, and precipitated insoluble Fe-OM complexes (Chen et al., 2014; Kleber et al., 2014). The high concentrations of DOC that often accumulate in paddy topsoils under anoxic conditions (Said-Pullicino et al., 2016) may favour the formation of aqueous organic Fe^{2+} complexes (Henneberry et al., 2012; Jones et al. 2015) that may precipitate and contribute to C retention during the formation of Fe-OM coprecipitates under subsequent oxic conditions.

Coprecipitation may result in different mineral surface properties (e.g. specific surface area, surface charge, particle aggregation/dispersion) with respect to adsorption (Mikutta et al., 2014), and may consequently affect the reactivity and stability of these Fe-OM associations (Chen et al., 2014; Euterhues et al., 2014). Recently, various studies have evaluated the mechanisms of formation, properties and reactivity of Fe-OM phases derived from coprecipitation with different OM sources, such as forest-floor DOM (Chen et al., 2014; Eusterhues et al., 2008, 2011; Mikutta et al., 2014), lignin and hydroxybenzoic acids (Eusterhues et al., 2011; Mikutta, 2011), humic and fulvic acids (Angelico et al., 2014; Pedròt at al., 2011; Shimizu et al., 2013), and polysaccharides (Mikutta et al., 2008). Depending on the DOM composition contrasting results have been reported as to whether coprecipitation actually leads to a greater C retention with respect to adsorption. Nonetheless, these works generally agree that the mechanisms involved, and the amount and selectivity of C retained during coprecipitation is highly dependent on the composition of the solution from which they precipitate. Most studies considered the coprecipitation of DOM during the hydrolysis of Fe^{3+}, but only a few studies have evaluate the coprecipitation process during the oxidation and hydrolysis of Fe^{2+} at circum-neutral pH, which is generally considered as the main process responsible for the formation of coprecipitates in soils subjected to alternating redox conditions. Moreover, few studies have evaluated this process in paddy soils where rice straw decomposition is the main contributor to the DOM pool.

Based on these considerations we hypothesized that during the oxidation and hydrolysis of Fe^{2+} in the presence of straw-derived DOM, (i) coprecipitation may lead to a greater retention of organic C with respect to surface adsorption; (ii) increasing amounts of DOC with respect to Fe (increasing initial C/Fe ratio) may favour the contribution of Fe-OM complexation and precipitation to the total C retained by coprecipitation, and also hinder the homogeneous nucleation of Fe (hydr)oxide nuclei, thus affecting the size and structure of the Fe (hydr)oxide formed; and (iii) the selective retention of particular organic constituents depends on the relative contribution of Fe-OM complexation and adsorption processes during coprecipitation. We tested these hypotheses by synthesizing a series of Fe-OM associations with increasing C/Fe ratios at pH = 6 prepared by either surface adsorption (SA) or coprecipitation (CP) of rice straw-derived DOM. In order to gain insights into the coprecipitation process we evaluated the kinetics of Fe^{2+} oxidation and complexation, and the total and selective retention of DOC. The synthesized associations were then characterized by physicochemical, spectroscopic and thermal analyses. A natural Fe-OM coprecipitate was also obtained by *in situ* sampling of paddy soil solutions from the anaerobic topsoil during a cropping season and subsequent oxidation in order to compare the obtained material with laboratory-synthesized coprecipitates.

2. Materials and Methods

2.1 Rice straw-derived dissolved organic matter extraction

Rice straw (cut into 1-2 cm segments) was soaked in deionized water (straw-solution ratio of 1:30), inoculated with a paddy soil extract (Haplic Gleysol, NW Italy) and incubated for 30 days at 25°C under oxic conditions to simulate field conditions after crop residue incorporation. Redox potential (Eh) and dissolved O_2 concentrations, determined potentiometically and polarographically respectively, were monitored regularly and adjusted by bubbling air through the suspension to ensure oxic conditions. A preliminary test showed that under these conditions straw extracts with a relatively high DOC concentration (≈ 450 mg C l^{-1}) and a significant proportion of aromatic constituents (specific UV absorption at 254 nm ≈ 1.8 l mg^{-1} m^{-1}) could be obtained. The suspension was filtered through 0.45 µm cellulose acetate filters and freeze-dried. Table 1 presents the chemical characteristics of the rice straw-derived DOM used in this study.

2.2 Synthesis of ferrihydrite and Fe-OM associations

Ferrihydrite (Fh) was prepared by rapidly oxidizing 2 l of a solution of 2 mM $FeCl_2$ at pH 6 in a stirred vessel by bubbling O_2 at a rate of 200 ml min^{-1} until complete oxidation evaluated through the disappearance of Fe^{2+} from solution. Considering the important influence of Si on the structure of ferrihydrite (Karim, 1984; Schwertmann and Thalmann, 1976), silicic acid was added before oxidation to obtain an Si concentration of 0.4 mM and an initial molar Si/Fe ratio of 0.2. This amount was equivalent to the maximum amount of Si present in the rice straw-derived DOM solutions used in this work. At this Si/Fe molar ratio the formation of green rust is inhibited and ferrihydrite is the ultimate oxidation product (Karim, 1986). During oxidation the pH was maintained at 6.0 by progressive addition of 0.25 M KOH by means of an automatic titrator (TTT85 titrator and ABU80 autoburette, Radiometer, Copenhagen, Denmark), and the additions of base were recorded.

Ferrihydrite-OM surface adsorbed systems (SA) with increasing C loadings were prepared by equilibrating DOM solutions having different initial C concentrations (20–260 mg C l^{-1}) with suspensions of Fh (previously prepared as described above) at pH 6.0 to obtain initial molar C/Fe ratios of 1, 5 and 10 (SA1, SA5 and SA10, respectively). Fe-OM coprecipitates (CP) with similar initial molar C/Fe ratios (CP1, CP5 and CP10, respectively) were prepared by oxidizing a solution of 2 mM $FeCl_2$ (under the same conditions as described above for Fh) in the presence of increasing amounts of DOC (20–260 mg C l^{-1}). Prior to oxidation, Si concentrations in the DOM solutions were adjusted to an initial Si/Fe ratio of 0.2.

All batch preparations (2 l total volume), performed in triplicate, were maintained under vigorous stirring for 4 h at 25°C (maximum time required for complete Fe(II) precipitation) and subsequently allowed to equilibrate for another 20 h at 4°C. Suspensions were then centrifuged, the residual DOM solution filtered through a 0.45 μm membrane filter for further analysis, and part of the solution freeze-dried. The amount of C retained was determined as the difference between initial and equilibrium DOC concentrations, while the selective retention of specific organic compounds was evaluated by determining the molar absorptivities of DOM solutions at 254 nm before (ε_0) and after adsorption/coprecipitation (ε). The influence of abiotic oxidation on changes in the chemical and spectroscopic properties of OM during coprecipitation was also evaluated by control trials on samples prepared bubbling O_2 in a solution of DOM in the absence of Fe^{2+}.
The synthesized adsorbates/coprecipitates were washed with deionized water, dialyzed through a 14 kDa membrane, shock-frozen by dropwise injection into liquid N_2 (-196 °C) in order to reduce the effect of freeze-compaction due to cryosuction (Hofmann et al., 2004), and finally freeze-dried, gently homogenized in an agate mortar and stored in a desiccator until analyses.

2.3 Field coprecipitate

The coprecipitates prepared *in vitro* were compared with a coprecipitate obtained from the soil solution collected *in situ* from a temperate paddy soil during rice cropping under continuous flooding. Before the beginning of the cropping season, multiple suction plates (25×25 cm; 0.45 μm pore size; EcoTech, Bonn, Germany) were installed horizontally at a depth of 25 cm (above the plough pan) in one of the continuously flooded plots of the Ente Nazionale Risi (NW Italy) experimental platform. Full details of the experimental site, design, as well as variations in DOC and Fe^{2+} concentrations and fluxes during the cropping season are provided elsewhere (Said-Pullicino et al., 2016). Soil solutions were sampled continuously by means of a suction pump for a period of about 3-5 days on three occasions (at tillering, panicle differentiation and ripening just before final field drainage) in correspondence with elevated DOC (20-60 mg C l^{-1}) and dissolved Fe^{2+} (20-65 mg Fe l^{-1}) concentrations. During sampling, N_2 was used as a shield gas to avoid Fe^{2+} oxidation and precipitation inside the sampling bottles. Aliquots of the collected solutions were analyzed for DOC and Fe^{2+} concentrations while the bulk of the solutions were oxidized in the lab and the precipitates formed separated by centrifugation, purified by dialysis and freeze-dried as described above. All field coprecipitates collected over the cropping season were joined into a single sample (CPf).

2.4 Coprecipitation kinetics

In order to understand the mechanisms that control the formation of Fe-OM coprecipitates as a function of time and initial C/Fe ratio, we evaluated the kinetics of the Fe^{2+} oxidation-hydrolysis process and retention of DOC. During the preparation of Fh and the three CP systems the addition of OH^-, the precipitation and complexation of Fe(II), as well as changes in the concentration and molar absorptivity of DOC were monitored. At regular time intervals a small aliquot of the reaction mixture was sampled, filtered through a 0.45 μm nylon membrane filter and analyzed for free and complexed Fe^{2+}, Fe^{3+}, DOC and UV absorption at 254 nm. At each sampling time, the volume of OH^- added by the automatic titrator was recorded. All concentrations were corrected for the volumes of base added and solution sampled.

2.5 Chemical and spectroscopic analyses of the solutions

Dissolved organic carbon was determined using Pt-catalyzed, high-temperature combustion (850°C) followed by infrared detection of CO_2 (VarioTOC, Elementar, Hanau, Germany), after removing inorganic C by acidifying to pH 2 and purging with CO_2-free synthetic air. The molar absorptivity (ε) of DOM solutions was determined by measuring the UV absorbance at 254 nm (Helios, Thermo Electron, Massachusetts, USA) and normalizing for the DOC concentration (Weishaar et al., 2003). Interference from aqueous Fe(III) complexes (Stefànsson, 2007) and Fe(III) oxyhydroxide colloids (Pullin and Cabaniss, 2003) at this wavelength were excluded from the absence of detectable concentrations of soluble Fe(III). Moreover, considering the low absorbance of soluble Fe(II) complexes at this wavelength (Doane and Horwàth, 2010), no correction of absorbance values was required. Dissolved Fe^{2+} concentrations were measured colorimetrically immediately after sampling using the 1,10-phenanthroline method (Loeppert and Inskeep, 1996). The absorbance of the tri-(1,10-phenanthroline) ferrous complex was measured after 30 min and 24 h as described by Gaffney et al. (2008). The former was a measure of free Fe^{2+} and the latter of total ferrous Fe in solution. The difference between the two measurements corresponded to the concentration of OM-complexed Fe(II). Dissolved Fe^{3+} contents were determined in a similar way after addition of hydroxylamine hydrochloride as a reducing agent. Fourier transform infrared (FTIR) spectra of DOM samples before and after adsorption or coprecipitation at pH 6.0 and 2.0 were acquired between 4000 and 400 cm^{-1} with a resolution of 4 cm^{-1} (PerkinElmer Spectrum 100, USA) on pellets obtained by pressing 2.0 mg of DOM with 200 mg of KBr. Chemical properties of DOM retained by adsorption and coprecipitation were evaluated through difference FTIR spectra obtain by subtracting the spectra of equilibrium DOM from that of the original DOM after appropriate spectra normalization.

2.6 Characterization of Fe-OM associations

The organic C content of the adsorbates and coprecipitates was determined by high temperature oxidation followed by infrared detection of CO_2 evolved (VarioTOC, Elementar), while Fe contents were determined by dissolution in concentrated HCl and quantification by atomic absorption spectroscopy (PerkinElmer AAnalyst 1400, USA) after appropriate dilution. X-ray diffraction (XRD) spectra were acquired (CuKα radiation, 45 kV, 40 mA) in Bragg-Brentano geometry between 10° to 70°, with a step size of 0.02°, and a 4 s step time (PANalytical X'Pert PRO MPD diffractometer, The Netherlands). The specific surface area (SSA) and porosity were determined by N_2 adsorption–desorption isotherms performed at 77 K by means of a surface area analyzer (ASAP 2020, Micrometrics, USA) after 24 h of outgassing at 303 K under vacuum (residual pressure 10^{-2} mbar) in order to remove all the gaseous contaminants adsorbed on the surface or within the porosity. The SSA was estimated by applying the Brunnauer–Emmet–Teller (BET) equation to the N_2 sorption data obtained in the relative pressure (p/p_0) range of 0.05 to 0.30 (Gregg and Sing, 1982). Pore volumes and pore size distributions were calculated by the density functional theory (DFT) method assuming slit-like geometry, while total pore volume was calculated from the volume of adsorbed N_2 at p/p_0 = 0.97. The mineral SSA ($m^2\ g^{-1}$) and pore volumes ($mm^3\ g^{-1}$) were corrected for the weight of retained OM as described by Mikutta et al. (2008). The zeta potential (ζ) was calculated from the electrophoretic mobility determined on a suspension of freshly synthesized material by Laser Doppler Velocimetry coupled with Photon Correlation Spectroscopy (LDV-PCS) using a spectrometer (DELSA 400, Beckman Coulter Inc., USA) equipped with a 5 mW He–Ne laser (632.8 nm). Thermogravimetric analyses (TGA) were performed in duplicate on Fh and Fe-OM associations as well as DOM samples with a heating ramp of 10 °C min^{-1} from 30 to 900 °C (TA Q600, TA instruments, USA). Sample amount (ca. 15 mg) was adjusted according to the C content of the analyzed materials as suggested by Fernàndez et al. (2012). Some measurements were replicated with a lower amount of sample in order to avoid oscillation due to fast release of gases. Modification of the hydroxide during TGA was

evaluated by XRD analysis of the residual matrices in spinner configuration and using a silicon support.

3. Results and discussion

3.1 Carbon retention by adsorption and coprecipitation

Carbon retention by adsorption on Fh tended to increase with increasing initial molar C/Fe ratios, gradually approaching a maximum at larger C/Fe ratios (Table 2) likely due to surface saturation of sorption sites. On a mass basis, sorption of straw-derived DOM on Fh prepared by oxidation of Fe^{2+} resulted in a maximum C content of 47 mg g^{-1} corresponding to C loading of 0.12 mg C m^{-2} Fh. This value is rather low compared to that (1.1 mg C m^{-2}) obtained by Kaiser et al. (2007) who evaluated the sorption of water-extractable OM obtained from forest-floor organic horizons (carboxyl acidity: 169 mmol mol^{-1} C) on a ferrihydrite produced by hydrolysis of Fe^{3+}. The relatively low surface loadings obtained in this work can probably be explained by the limited reactivity of the straw-derived OM (carboxyl acidity: 23 mmol mol^{-1} C), as well as the different properties of the Fh synthesized by Fe^{2+} oxidation and hydrolysis (discussed later).

In contrast, molar C/Fe ratios of coprecipitates increased linearly with increasing initial molar C/Fe ratios (r^2 = 0.996) over the experimental range evaluated (up to C/Fe = 10), suggesting that maximum C retention was not reached under the experimental conditions studied. The highest C content of 213 mg C g^{-1} obtained for CP10 (Table 2) was ~4.5 times higher than the amount of C retained by adsorption at the same initial C/Fe ratio. In fact, whereas C contents and molar C/Fe ratios of adsorption and coprecipitation products were similar at an initial molar C/Fe ratio of 1, higher values were obtained for coprecipitates than adsorption complexes at initial molar C/Fe ratios > 5 (Table 2). These results are in line with the observations reported by Chen et al. (2014) who found a greater retention of forest floor-derived DOC through coprecipitation with respect to adsorption at initial molar C/Fe ratios > 3.8, and C contents in the coprecipitates of ~290 mg C g^{-1} at an initial molar C/Fe ratio of ~10. In contrast, Eusterhues et al. (2011) found that coprecipitation of a forest floor water extract with Fe (initial molar C/Fe ≈ 10) yielded a maximum C content similar to adsorption. However, they also found that coprecipitation could retain twice more C than adsorption when lignin was used at an initial molar C/Fe ratio of 18. These results suggest that apart from initial C/Fe ratio, the composition of OM is another key factor determining the relative retention of C by coprecipitation with respect to adsorption. Consequently, this suggests that coprecipitation is expected to influence the amount and composition of DOM remaining in solution, as evidenced and discussed later.

The field coprecipitate (CPf) showed a slightly lower C content (C/Fe = 0.8) with respect to the synthesized coprecipitates, considering that the mean initial C/Fe ratio of 3.5 was intermediate between CP1 and CP5 (Table 2), further suggesting that DOM composition greatly influenced the C retention. When compared to adsorption products, the field coprecipitate nonetheless showed a higher C content.

Variations in the relative molar UV absorbance at 254 nm of DOM after adsorption on Fh showed values of $\varepsilon/\varepsilon_0 < 1$ at low initial DOC concentration (Table 2), suggesting a slight preferential retention of aromatic constituents during the sorption of DOM on Fe (hydr)oxides (Mikutta et al., 2007). Sodano et al. (2016) found a good correlation between selective retention of aromatic constituents and microporosity of the Fe (hydr)oxide that was attributed to a higher occupation of the micropores by the smaller aromatic components. Considering the low microporosity of the Fh produced by oxidation of Fe^{2+}, this could explain the rather limited selective retention of aromatic constituents during adsorption. In contrast, coprecipitation resulted in a stronger affinity for aromatic constituents with respect to adsorption, particularly at lower initial C/Fe ratios, as evidenced by $\varepsilon/\varepsilon_0$ values ranging from 0.1 to 0.7 (Table 2). Similar results were obtained by Henneberry et al. (2012) who observed a preferential complexation of more aromatic, higher molecular weight material, rich in carboxylic

functional groups during coprecipitation. These results suggest that the higher retention of C during coprecipitation with respect to adsorption may not necessarily be due to a non-selective, physical occlusion of organic constituents within the forming coprecipitate but involves a selective chemical interaction between specific constituents of DOM and the precipitating Fe.

3.2 Coprecipitation kinetics and selective retention of DOC

The kinetics of the coprecipitation process evidenced a decrease in the rate of Fe^{2+} oxidation and precipitation with increasing initial C/Fe ratios (Fig. 1). In fact, the time required for total Fe^{2+} oxidation and precipitation ranged from 25 min in the absence of OM to 210 min for CP10. This is in agreement with the widely held notion that organic substances can affect the rate of Fe^{2+} oxidation in the presence of dissolved oxygen. This influence depends on the rate constants of Fe(II) complexation, and the relative rate constants of Fe(II) and Fe(II)-OM oxidation (Jones et al., 2015; Rose and Waite, 2003; Theis and Singer, 1974). Theis and Singer (1974) and Jones et al. (2015) suggested that the formation of strong Fe^{2+} complexes with simple aliphatic carboxylic acids, such as citric acid, might increase the rate of oxidation. In contrast, Fe^{2+} oxidation was also shown to be hindered by the presence of water soluble natural organic matter extracted from pine litter (Rose and Waite, 2003) or derived from the decay of natural vegetation (Theis and Singer, 1974). Considering that pH was maintained constant during oxidation, we hypothesise that the slower rates of Fe^{2+} oxidation in the presence of increasing amounts of straw-derived DOM was due to the predominant formation of stable Fe(II)-OM complexes having lower oxidation rate constants with respect to uncomplexed Fe(II). We cannot however exclude that Fe^{2+} adsorption onto the newly formed poorly crystalline Fe(III) (hydr)oxides, that could have also contributed to the decreasing solution Fe^{2+} concentrations (Thompson et al., 2006b), was probably greater at lower C loadings.

The measured rates of OH^- consumption showed a similar trend to those observed for Fe^{2+} oxidation (Fig. 2). However, with increasing C/Fe ratios, the total amount of OH^- consumed deviated from stoichiometric values for the oxidation and hydrolysis of Fe^{2+} (molar OH^-/Fe^{2+} ratio <2). This was attributed to the formation and precipitation of Fe-OM complexes (Fig. 1), although an effect of the buffering capacity of the added DOM, proton sorption at particle surfaces, and release of OH^- from the (hydr)oxide surface due to OM sorption by ligand exchange cannot be excluded (Thompson et al., 2006b) . During Fe^{2+} oxidation, interaction with negatively charged carboxylic and phenolic functional groups of DOM could have involved both ligand exchange at the surface of the newly formed Fe-hydroxide nuclei, as well as electrostatic attraction (in competition with hydroxyl ions) and complexation with soluble Fe^{2+} cations. The latter process was confirmed by the presence of soluble Fe(II)-OM complexes throughout the oxidation in CP10 and, to a lesser extent, towards the initial stages of oxidation in CP1 and CP5 (Fig. 1). CP10 was indeed characterized by an instantaneous precipitation of around 20% of initial Fe at the beginning of the experiment ($Fe/Fe_0 = 0.2$ at $t = 0$), as well as the formation of important amounts of complexed Fe^{2+} in solution during the coprecipitation process (Fig. 1). In line with the findings of Thompson et al. (2006b), the absence of significant concentrations of Fe^{3+} in the solution throughout the oxidation in all systems (data not shown), suggested that Fe^{2+} oxidation resulted in its immediate precipitation, and that all soluble Fe-OM complexes involved exclusively Fe^{2+}.

The kinetics of C retention during coprecipitation, expressed as the absolute amount of C retained, and molar C/Fe ratio of the coprecipitates formed are shown in Fig. 3a and b, respectively, while the selective retention of aromatic constituents evaluated through the relative molar UV absorbance of DOM is shown in Fig. 3c. All kinetics generally showed an initial rapid retention of C on the formed coprecipitate that tended to reach an equilibrium as the Fe^{2+} in solution disappeared. Control trials with DOM alone did not evidence any measurable loss of C or variations in $\varepsilon/\varepsilon_0$ during oxidation. In CP1 the amount of retained C tended to increase gradually with time as Fe^{2+} was oxidized, and a

coprecipitate with a relatively constant C/Fe ratio ranging between 0.4 and 1.1 was formed (Fig. 3a and b). At the beginning of the oxidation, the small amount of Fe(II)-OM complexes determined (Fig. 1) did not lead to a measurable retention of DOC (Fig. 3a). Retained DOC was indeed less than 0.2 mmol C suggesting that C retention was not driven by the formation and subsequent oxidation and precipitation of these complexes. Maximum C retention was observed after ~40 min, which coincided with the complete precipitation of Fe^{2+}. $\varepsilon/\varepsilon_0$ decreased rapidly from values ≈1.2 to 0.1 suggesting a preferential retention of aromatic constituents (Fig. 3c).

At higher initial C/Fe ratios, variations in the concentrations of Fe^{2+} and DOC with time suggested that coprecipitation could actually involve the formation of different Fe-OM associations following different kinetics. At the beginning of the oxidation, initial Fe precipitation was accompanied by a rapid increase in retained DOC that seemed to slow down and approach a maximum after 10 and 20 min for CP5 and CP10, respectively (Fig. 3a). During this initial stage, the coprecipitates formed had a relatively high C/Fe ratio ranging between 3.4-7.2 and 5.1-9.4 for CP5 and CP10, respectively. These results seem to suggest that the main process driving the initial C retention involved a direct association between soluble Fe^{2+} ions and C functional groups followed by a rapid oxidation and precipitation of Fe-OM complexes rich in C (Fig. 1), rather than the sorption of OM on the surface of a newly forming Fe hydroxide mineral phase (Henneberry et al., 2012). Moreover, the initial increase in $\varepsilon/\varepsilon_0$ to values > 1 over this period suggests that aliphatic constituents are the first to be depleted from solution possibly due to their preferential complexation with Fe^{2+} and subsequent oxidation and precipitation as Fe^{3+} salts (Fig. 3c; Schnitzer and Skinner, 1964). This hypothesis was further confirmed by the concurrence of a second accumulation of complexed Fe(II)-OM at around 90 min in CP10 (Fig. 1), together with a slight relative increase in $\varepsilon/\varepsilon_0$ values (Fig. 3c). Pham and Waite (2008a, b) observed that the number of anions involved in the Fe-OM complex may affect the rate of Fe oxidation, further explaining the acceleration in oxidation kinetics with a decreasing C/Fe ratio in solution. Although coprecipitation was initially driven by a selective retention of aliphatic compounds, $\varepsilon/\varepsilon_0$ values were < 1 after 5 and 20 min for CP5 and CP10, respectively. We hypothesize that subsequent retention of DOC during coprecipitation in CP5 and CP10 probably involved both salt precipitation and OM sorption on the forming mineral phase through the preferential interaction with aromatic constituents. Sorption processes seemed to dominate when the coprecipitates showed a lower and rather constant C/Fe ratio (Fig. 3).

The kinetics of the coprecipitation processes therefore suggested that the higher C retention obtained by coprecipitation with respect to adsorption at high initial C/Fe ratios was probably due to an initial complexation of Fe^{2+} by low molecular weight aliphatic carboxylic acids followed by oxidation and precipitation as C-rich metal salts apart from the adsorption of OM on Fe hydroxide. This implies that the relative proportion of C retained by metal complexation and precipitation with respect to OM sorption, as well as the process-related selectivity for particular organic constituents could control the total C retention during coprecipitation. This also explains why comparative evaluation of C retention by surface adsorption and coprecipitation processes strongly depends on the source and chemical composition of DOM, and the method of preparation of the Fe hydroxides.

3.3 X-ray diffraction, specific surface area, porosity and surface charge

The XRD diffractogram of OM-free Fh formed during the oxidation of Fe^{2+} showed two weak reflexes at d = 0.26 and 0.15 nm characteristic of 2-line ferrihydrite (Fig. 4). The broad nature of these peaks and the absence of peak shoulders suggest that crystals of Fh synthesized by this method has low range crystallinity and a reduced size with respect to ferrihydrite prepared by hydrolysis of Fe^{3+} (Eusterhues et al., 2008). Moreover, the presence of Si in the initial solution could also be responsible for hindering the crystal growth. With increasing C loading, the XRD pattern of the coprecipitates showed a progressive broadening of the main peaks, until they disappeared completely for CP10 (Fig. 4). At

higher initial C/Fe ratios, the formation of Fe(II)-OM complexes (Fig. 1) could have promoted the interaction between Fe $(O, OH)_6$ octahedra and organic molecules, and precipitation of an OM-rich Fh particles. This phenomenon could have prevented subsequent cross-linking between chains of Fe octahedra leading to a decrease in the size of coherent scattering domains or an increase in stacking disorder (Eusterhues et al., 2008). Similarly, Gaffney et al. (2008) showed that in the absence of OM, ferrihydrite crystal grows during Fe^{2+} oxidation through a homogeneous nucleation of Fe hydroxide nuclei, providing surface sites for autocatalytic Fe^{2+} oxidation that induces growth of a Fe(III) layer on the hydroxide surface. However, in the presence of OM, DOC sorption on newly formed Fe hydroxide particles was reported to result in a non-homogeneous nucleation consequently leading to a slower crystal growth. The presence of Si could also contribute to the inhibition of the autocatalytic oxidation of Fe^{2+} (Kinsela et al., 2016). Similar XRD diffractograms were obtained for CPf (Fig. 4), except for an additional reflection at 0.33 nm probably due to Fe-phosphate precipitates (Voegelin et al., 2013), thus suggesting that the synthesized Fe-OM coprecipitates were similar to those formed under natural conditions.

The OM-free Fh had a SSA of 385 $m^2\ g^{-1}$, a total pore volume of 418 $mm^3\ g^{-1}$, and a N_2-detected microporosity that contributed to only 4% of the total pore volume (Table 3). Whereas the measured SSA accords well with published data (Cornell and Schwertmann, 2003; Eusterhues et al., 2008; Hofmann et al., 2004; Mikutta et al., 2008; Mikutta et al., 2014), Fh prepared by Fe^{2+} oxidation had a high total pore volume but a very limited micropore volume with respect to those reported for 2-L ferrihydrite prepared by hydrolysis of Fe^{3+} (total and micropore volume between 157-266 and 39-149 $mm^3\ g^{-1}$, respectively; Chen et al., 2014; Mikutta et al., 2008; Mikutta et al., 2014; Poggenburg et al., 2016). This suggests that oxidation of Fe^{2+} forms ferrihydrite aggregates composed of small particles with a diameter < 4 nm, assuming a density of ~4 $g\ cm^{-3}$ (Cornell and Schwertmann, 2003), a spherical geometry and no surface roughness.

Sorption of OM onto the Fh surface generally resulted in a decrease in N_2 SSA and total pore volume (24 and 19% for the SA10 at highest C loading, respectively; Table 3). This was mainly due to the formation of denser aggregates by the association with OM, and the masking of the mineral surface by OM having a very low N_2 BET SSA (~1 $m^2\ g^{-1}$; Eusterhues et al., 2008). The expected preferential loss of N_2-accessible micropores with increasing OM sorption with respect to mesopores due to the preferential sorption of OM at micropore openings (Kaiser et al., 2007) was not observed, probably related to the limited microporosity of the Fh and low acidity of the OM used. The only exception to this trend was observed for SA5 that showed higher SSA, micro and mesopore volume than SA1, notwithstanding a higher OM content (compare the values in Table 2 and 3). This behaviour has been explained considering a possible dispersion of Fh particles as a consequence of OM sorption (Sodano et al., 2016), exposing Fh surfaces for N_2 sorption.

Likewise, all coprecipitates had a significantly reduced SSA compared to OM-free Fh (Table 3). The mineral SSA of CP1 was 12% less with respect to that of OM-free Fh, and decreased up to 85 to 88% in CP5 and CP10, respectively. While the presence of OM during the formation of ferrihydrite is known to inhibit crystallization due to specific adsorption onto nucleation sites responsible for crystal growth (Mikutta et al., 2008), coprecipitation may also favour substantial particle aggregation as evidenced by the decrease in N_2 SSA, and micro- and small mesopore (2-10 nm) volume with increasing C contents (Table 3). Compared to OM-free Fh, up to 87% of mineral 2-10 nm mesopore volume was lost by coprecipitation at highest C content, whereas the 10-50 nm mesopore volume increased by 17%. These results, also observed for the field coprecipitate, suggest a strong aggregation of particles with coprecipitation. Similar results were observed for the precipitation of ferrihydrite via hydrolysis in the presence of polysaccharides (Mikutta et al., 2008) or humic acids (Shimizu et al., 2013).

The ζ potential of freshly formed Fe-OM associations at pH 6 also contributed to understand the different mechanisms of C retention by adsorption and coprecipitation (Table 3). Fh had a positive

surface charge (+28 mV) only slightly lower than typical values (Celi et al., 2003) probably due to its Si content (Anderson and Benjamin, 1985). As expected, OM adsorption on the positive Fh surface led to the formation of a net negative surface charge even at the lowest C contents (-18 mV for SA1). The ζ potential tended to decrease with increasing C loadings reaching values as low as -44 mV for SA10, indicating that the surface retained OM had a high number of negatively charged functional groups not involved in adsorption bonding. The less negative surface charge observed for SA5 with respect to SA1 was probably a result of the dispersion of positive Fh particles, in agreement with the observed increase in SSA. Notwithstanding the higher C contents, ζ potentials of the coprecipitates were less negative with respect to the adsorbed systems (Table 3). In fact, CP10 had a less negative surface charge than SA10 despite retaining 4.5 times more organic C. This suggests that during coprecipitation negatively charged functional groups of retained OM not immediately involved in bonding with Fe, were eventually neutralized by further interaction with Fe, supporting the formation of highly aggregated Fe-OM associations with significant amounts of included OM. Thus, these differences in the effect of coprecipitation with respect to adsorption on particle aggregation and surface charge could have important implications on the colloidal dispersion/aggregation equilibrium (cf. Thompson et al., 2006a) and consequently C mobilization (cf. Buettner et al., 2014) in soils subjected to alternating redox conditions.

3.4 Fourier-transform infrared spectroscopy

FTIR spectra of OM-free Fh (data not reported) showed the characteristic pattern of 2-line ferrihydrite (Cornell and Schwertmann, 2003) except for the presence of an additional band at 950 cm^{-1} characteristic of Fe-O-Si interactions (Carlson and Schwertmann, 1981) due the incorporation of Si into the structure. Further insights into the selective retention of DOC during adsorption and coprecipitation were obtained by evaluating difference FTIR spectra of the Fe-OM associations at the highest C loadings (SA5 and SA10, and CP5 and CP10, respectively; Fig. 5). Adsorption resulted in a greater retention of aryl methoxy (2855 cm^{-1}) and methyl (2964 and 2930 cm^{-1}) substituents on aromatic molecules (Fig. 5). The presence of peaks corresponding to the asymmetric (1570 cm^{-1}) and symmetric (1423 cm^{-1}) stretching of aryl -COO^- groups, and shoulders at 1460, 1457 and 1450 cm^{-1} attributable to Ar-O-CH_3 vibrations suggest that sorption involved a selective retention of lignin-derived phenols through interaction with aromatic carboxylic constituents. In contrast, coprecipitation also resulted in a greater retention of methyl (2974 cm^{-1}) or methylene (2941 cm^{-1}) substituents on aliphatic or saccharide constituents with respect to adsorption (Fig. 5). Positive peaks at 1587 and 1402 cm^{-1} corresponding to asymmetric and symmetric stretching of alkyl-COO^- groups respectively, suggested that coprecipitation also involved the formation of Fe complexes with aliphatic carboxylic groups. Moreover, difference spectra of CP5 and CP10 showed negative absorption bands around 1611, 1533 and 674 cm^{-1} corresponding to N-H deformation of primary and secondary amines. Reasonably, positively charged functional groups were selectively excluded from the complexation process with Fe^{2+} because of electrostatic repulsion. This was particularly evident in the coprecipitates because of the much higher amount of OM retained compared to adsorbed systems.

3.5 Thermogravimetric analysis

Thermogravimetric (TG) mass losses were observed at different temperature ranges depending on the initial C/Fe ratio in both adsorbed and coprecipitated systems (Fig. 6). The contribution of Fh dehydration to mass loss over the temperature range considered was negligible (Fig. 6a), possibly because the presence of Si within the Fh structure weakens and broadens the peak relative to its crystallization into haematite (Campbell et al., 2002; Carlson and Schwertamann, 1981). TG and differential TG (DTG) curves of the straw-derived DOM used in this work showed a small peak near 50 °C due to the loss of residual water, and other two peaks with maxima at 360 and 445 °C relative to decomposition reactions (Fig. 6a and c). Mass loss at a temperature range between 250-280 °C was attributed to OM decarboxylation reactions (Escudey et al., 1999; Provenzano and Senesi, 1999; Schnitzer and Hoffman, 1966). The low temperature part of the exothermic region around 300-350 °C has been generally attributed to the oxidation of carbohydrates and other aliphatic compounds, while peaks with maxima around 400-450 °C are thought to result from the decomposition of more aromatic compounds such as lignin-derived phenols or other polyphenols (Dell'Abate et al., 2002; Strezov et al., 2004).

Apart from low temperature dehydration reactions, SA systems only evidenced a single peak in the temperature range relative to OM degradation reactions, with a maximum shifted to a slightly lower temperature (~340 °C) with respect to the original DOM (Fig. 6a and c). With increasing C loadings total weight loss at 650 °C increased from 18 to 23 % from Fh to SA10, and DTG peak maxima due to OM decomposition were slightly shifted to lower temperatures as a result of interaction with Fh (Fig. 6c).

Even CP systems showed a single mass loss over the OM degradation temperature range (Fig. 6b), although DTG peak maxima were shifted to even lower temperatures (~325 °C), and weight loss was distributed over a larger temperature range with respect to SA systems, especially for CP5 and CP10 (Fig 6d). The field coprecipitate showed a TG curve similar to those obtained for the synthesized coprecipitates. These results suggest that with increasing OM contents the contribution of decarboxylation and oxidation of low molecular weight aliphatic compounds tended to increase. Moreover, OM decarboxylation, possibly responsible for peak shoulders at 270 and 258 °C for CP5 and CP10 respectively (Fig. 6d), was observed at lower temperatures with respect to free DOM (Fig. 6c). Schnitzer and Skinner (1964) mainly attributed the shift to lower temperatures to the presence of Fe-OM complexes, although a catalytic effect of the metal on decarboxylation reactions could not be excluded.

Analysis of CP5 and CP10 samples utilizing ~15 mg aliquots (rather than 6-7 mg when the higher C content of these systems was taken into account) produced the TG curves reported in Fig. 6e. The higher amount of OM resulted in an analytical artefact observed as a sharp mass loss at a temperature between 243 and 275 °C accompanied with a slight temperature decrease. Nonetheless, this artefact seemed to confirm the precipitation of aliphatic Fe-OM salts during the first phases of coprecipitation and subsequent growth of Fe (hydr)oxides around these first nuclei. In fact, we speculate that the sharp loss in mass (causing a small vibration in the microbalance and decrease in temperature) could be attributed to the sudden evolution of CO_2 generated from the oxidation of aliphatic OM constituents located within the coprecipitate structure.

The XRD analysis of TG residuals for all systems showed characteristic peaks of a hematite phase (data not shown), confirming the presence of ferrihydrite even in the coprecipitates with highest C loading (i.e. CP5 and CP10).

4. Conclusions

Although the importance of Fe (hydr)oxides for C retention by surface adsorption is well known, only recently has coprecipitation been recognized as an important process responsible for C storage particularly in hydromorphic soils. Our results show that coprecipitation during the oxidation and hydrolysis of Fe^{2+} in the presence of rice straw-derived DOM resulted in a much higher C retention with respect to surface adsorption, with important amounts of OM included within the highly aggregated Fe-OM association formed. Coprecipitates sampled *in situ* also showed a similar retention of organic C confirming that this process may contribute significantly to the OM stabilization in paddy topsoils. However, further research is required to establish if OM retained by coprecipitation in soils experiencing frequent redox fluctuations is actually protected against microbial decomposition and thus contributes to the long-term accumulation of C in paddy soils.

The mechanisms involved in the retention of straw-derived DOM during coprecipitation were shown to be strongly dependent on C/Fe ratio of the solution. Although the overall coprecipitation process was highly selective for aromatic constituents, initial complexation of Fe^{2+} and precipitation as C-rich metal salts involved the selective interaction with aliphatic carboxylic constituents. The contribution of the latter mechanism to total C retention during coprecipitation was shown to increase with increasing solution C/Fe ratios. The process-related selectivity of specific constituents of DOM during coprecipitation highlights the involvement of specific mechanisms, i.e. complexation, adsorption, salt precipitation, while ruling out non-selective, physical occlusion of OM within the forming coprecipitate.

The fact that coprecipitation may represent a key process in controlling DOC retention is of particular interest for our understanding of stabilization mechanisms and turnover rates of certain classes of compounds, with important implications on the C source/sink functions of paddy soils.

Acknowledgements

This study was part of the project "Carbon source/sink functions of rice agro-ecosystems and implications for mitigating green-house gas emissions (CarboPAD)" funded by the 'Ministero dell'Istruzione, dell' Università e della Ricerca' (MIUR) within the framework 'Futuro in Ricerca 2013'. Luisella Celi and Daniel Said-Pullicino also acknowledge partial funding from the FACCE-JPI project "Greenhouse gas emissions from paddy rice soils under alternative irrigation management (GreenRice)". We also thank Marco Romani and Eleonora Miniotti at 'Ente Nazionale Risi' for their help in sampling the large volumes of soil solution necessary for obtaining the field coprecipitates.

References

Anderson, P.R., Benjamin, M.M., 1985. Effects of silicon on the crystallization and adsorption properties of ferric oxides. Environ. Sci. Technol. 19, 1048-1053.

Angelico, R., Ceglie, A., He, J.Z., Liu, Y.R., Palumbo, G., Colombo, C., 2013. Particle size, charge and colloidal stability of humic acids coprecipitated with ferrihydrite. Chemosphere 99, 239-247.

Baldock, J.A., Masiello, C.A., Gélinas, Y., Hedges, J.I., 2004. Cycling and composition of organic matter in terrestrial and marine ecosystems. Marine Chemistry 92, 39-64.

Buettner, S.W., Kramer, M.G., Chadwick, O.A., Thompson, A., 2014. Mobilization of colloidal carbon during iron reduction in basaltic soils. Geoderma 221-222, 139-145.

Campbell, A.S., Schwertmann, U., Stanjek, H., Friedl, J., Kyek, A., Campbell, P.A., 2002. Si incorporation into hematite by heating Si-ferrihydrite. Langmuir 18, 7804-7809.

Carlson, L., Schwertmann, U., 1981. Natural ferrihydrites in surface deposits from Finland and their association with silica. Geochim. Cosmochim. Acta 45, 421-425,427-429.

Celi, L., De Luca, G., Barberis, E., 2003. Effects of interaction of organic and inorganic P with ferrihydrite and kaolinite-iron oxide systems on iron release. Soil Sci. 168, 479-488.

Chen, C., Dynes, J.J., Wang, J., Sparks, D.L., 2014. Properties of Fe-organic matter associations via coprecipitation versus adsorption. Environ. Sci. Technol. 48, 13751-13759.

Cornell, R. M., Schwertmann, U., 2003. The iron oxides. Structure, properties, reactions, occurrences and uses. Second ed. Wiley-VCH, Weinheim, Germany.

Dell'Abate, M.T., Benedetti, A., Brookes, P.C., 2003. Hyphenated techniques of thermal analysis for characterisation of soil humic substances. J. Sep. Sci. 26, 433-440.

Doane, T.A., Horwath, W.R., 2010. Eliminating interference from iron(III) for ultraviolet absorbance measurements of dissolved organic matter. Chemosphere 78, 1409-1415.

Escudey, M., Díaz, P., Galindo, G., Chang, A.C., 1999. Differential thermogravimetric analysis of oxalate in hydrogen peroxide- treated allophanic soils. Commun. Soil Sci. Plant Anal. 30, 937-946.

Eusterhues, K., Rumpel, C., Kögel-Knabner, I., 2005. Stabilization of soil organic matter isolated via oxidative degradation. Org. Geochem. 36, 1567-1575.

Eusterhues, K., Wagner, F.E., Häusler, W., Hanzlik, M., Knicker, H., Totsche, K.U., Kögel-Knabner, I., Schwertmann, U., 2008. Characterization of ferrihydrite-soil organic matter coprecipitates by X-ray diffraction and Mössbauer spectroscopy. Environ. Sci. Technol. 42, 7891-7897.

Eusterhues, K., Rennert, T., Knicker, H., Kögel-Knabner, I., Totsche, K.U., Schwertmann, U., 2011. Fractionation of organic matter due to reaction with ferrihydrite: Coprecipitation versus adsorption. Environ. Sci. Technol. 45, 527-533.

Eusterhues, K., Hadrich, A., Neidhardt, J., Kusel, K., Keller, T.F., Jandt, K.D., Totsche, K.U., 2014. Reduction of ferrihydrite with adsorbed and coprecipitated organic matter: Microbial reduction by *Geobacter bremensis* vs. abiotic reduction by Na-dithionite. Biogeosciences 11, 4953-4966.

Fernàndez, J.M., Peltre, C., Craine, J.M., Plante, A.F., 2012. Improved characterization of soil organic matter by thermal analysis using CO_2/H_2O evolved gas analysis. Environ. Sci. Technol. 46, 8921-8927.

Gaffney, J.W., White, K.N., Boult, S., 2008. Oxidation state and size of Fe controlled by organic matter in natural waters. Environ. Sci. Technol. 42, 3575-3581.

Gregg, S.J., Sing, K.S.W., 1982. Adsorption, Surface Area and Porosity. Academic Press, London.

Henneberry, Y.K., Kraus, T.E.C., Nico, P.S., Horwath, W.R., 2012. Structural stability of coprecipitated natural organic matter and ferric iron under reducing conditions. Org. Geochem. 48, 81-89.

Hofmann, A., Pelletier, M., Michot, L., Stradner, A., Schurtenberger, P., Kretzschmar, R., 2004. Characterization of the pores in hydrous ferric oxide aggregates formed by freezing and thawing. J. Colloid Interf. Sci. 271, 163-173.

Jones, A.M., Griffin, P.J., Waite, T.D., 2015. Ferrous iron oxidation by molecular oxygen under acidic conditions: The effect of citrate, EDTA and fulvic acid. Geochim. Cosmochim. Acta 160, 117-131.

Kaiser, K., Guggenberger, G., 2000. The role of DOM sorption to mineral surfaces in the preservation of organic matter in soils. Org. Geochem. 31, 711-725.

Kaiser, K., Mikutta, R., Guggenberger, G., 2007. Increased stability of organic matter sorbed to ferrihydrite and goethite on aging. Soil Sci. Soc. Am. J. 71, 711-719.

Karim, Z., 1984. Characteristics of ferrihydrites formed by oxidation of $FeCl_2$ solutions containing different amounts of silica. Clay. Clay Miner. 32, 181-184.

Karim, Z., 1986. Formation of ferrihydrite by inhibition of green rust structures in the presence of silicon. Soil Sci. Soc. Am. J. 50, 247-250.

Kinsela, A.S., Jones, A.M., Bligh, M.W., Pham, A.N., Collins, R.N., Harrison, J.J., Wilsher, K.L., Payne, T.E., Waite, T.D., 2016. Influence of dissolved silicate on rates of Fe(II) oxidation. Environ. Sci. Technol. 50, 11663-11671.

Kleber, M., Eusterhues, K., Keiluweit, M., Mikutta, C., Mikutta, R., Nico, P.S., 2015. Mineral-organic associations: Formation, properties, and relevance in soil environments. Adv. Agron. 130, 1-140.

Kögel-Knabner, I., Amelung, W., Cao, Z., Fiedler, S., Frenzel, P., Jahn, R., Kalbitz, K., Kölbl, A., Schloter, M., 2010. Biogeochemistry of paddy soils. Geoderma 157, 1-14.

Loeppert, R.H., Inskeep, W.P., 1996. Iron. *In:* Bigham, J.M. (ed) Methods of Soil Analysis. Part 3. Chemical Methods. SSSA, Madison, Wisconsin, USA. pp. 639-664.

Mikutta, C., Mikutta, R., Bonneville, S., Wagner, F., Voegelin, A., Christl, I., Kretzschmar, R., 2008. Synthetic coprecipitates of exopolysaccharides and ferrihydrite. Part I: Characterization. Geochim. Cosmochim. Acta 72, 1111-1127.

Mikutta, C., 2011. X-ray absorption spectroscopy study on the effect of hydroxybenzoic acids on the formation and structure of ferrihydrite. Geochim. Cosmochim. Acta 75, 5122-5139.

Mikutta, R., Mikutta, C., Kalbitz, K., Scheel, T., Kaiser, K., Jahn, R., 2007. Biodegradation of forest floor organic matter bound to minerals via different binding mechanisms. Geochim. Cosmochim. Acta 71, 2569-2590.

Mikutta, R., Lorenz, D., Guggenberger, G., Haumaier, L., Freund, A., 2014. Properties and reactivity of Fe-organic matter associations formed by coprecipitation versus adsorption: Clues from arsenate batch adsorption. Geochim. Cosmochim. Acta 144, 258-276.

Pédrot, M., Boudec, A.L., Davranche, M., Dia, A., Henin, O., 2011. How does organic matter constrain the nature, size and availability of Fe nanoparticles for biological reduction? J. Colloid Interf. Sci. 359, 75-85.

Pham, A.N., Waite, T.D., 2008a. Oxygenation of Fe(II) in the presence of citrate in aqueous solutions at pH 6.0-8.0 and 25 °C: Interpretation from an Fe(II)/citrate speciation perspective. J. Physical Chem. A 112, 643-651.

Pham, A.N., Waite, T.D., 2008b. Modeling the kinetics of Fe(II) oxidation in the presence of citrate and salicylate in aqueous solutions at pH 6.0-8.0 and 25°C. J. Phys. Chem. A 112, 5395-5405.

Poggenburg, C., Mikutta, R., Sander, M., Schippers, A., Marchanka, A., Dohrmann, R., Guggenberger, G., 2016. Microbial reduction of ferrihydrite-organic matter coprecipitates by *Shewanella putrefaciens* and *Geobacter metallireducens* in comparison to mediated electrochemical reduction. Chem. Geol. 447, 133-147.

Provenzano, M.R., Senesi, N., 1999. Thermal properties of standard and reference humic substances by differential scanning calorimetry. J. Therm. Anal. Calorim. 57, 517-526.

Pullin, M.J., Cabaniss, S.E., 2003. The effects of pH, ionic strength, and iron-fulvic acid interactions on the kinetics of non-photochemical iron transformations. I. Iron(II) oxidation and iron(III) colloid formation. Geochim. Cosmochim. Acta 67, 4067-4077.

Rose, A.L., Waite, T.D., 2003. Effect of dissolved natural organic matter on the kinetics of ferrous iron oxygenation in seawater. Environ. Sci. Technol. 37, 4877-4886.

Said-Pullicino, D., Miniotti, E.F., Sodano, M., Bertora, C., Lerda, C., Chiaradia, E.A., Romani, M., Cesari de Maria, S., Sacco, D., Celi, L., 2016. Linking dissolved organic carbon cycling to organic carbon fluxes in rice paddies under different water management practices. Plant Soil 401, 273-290.

Schnitzer, M., Hoffman, I., 1966. A thermogravimetric approach to the classification of organic soils. Soil Sci. Soc. Am. Proc. 30, 63-66.

Schnitzer, M., Skinner, S.I.M., 1964. Organo-metallic interactions in soils: 3. Properties of iron- and aluminum-organic-matter complexes, prepared in the laboratory and extracted from a soil. Soil Sci. 98, 197-203.

Schwertmann, U., Thalmann, H., 1976. The influence of [Fe (II)],[Si], and pH on the formation of lepidocrocite and ferrihydrite during oxidation of aqueous $FeCl_2$ solutions. Clay Miner. 11, 189-200.

Schwertmann, U., 1991. Solubility and dissolution of iron oxides. Plant and Soil 130, 1-25.

Shimizu, M., Zhou, J., Schröder, C., Obst, M., Kappler, A., Borch, T., 2013. Dissimilatory reduction and transformation of ferrihydrite-humic acid coprecipitates. Environ. Sci. Technol. 47, 13375-13384.

Sodano, M., Said-Pullicino, D., Fiori, A.F., Catoni, M., Martin, M., Celi, L., 2016. Sorption of paddy soil-derived dissolved organic matter on hydrous iron oxide-vermiculite mineral phases. Geoderma 261, 169-177.

Stefánsson, A., 2007. Iron(III) hydrolysis and solubility at 25°C. Environ. Sci. Technol. 41, 6117-6123.

Strezov, V., Moghtaderi, B., Lucas, J.A., 2004. Computational calorimetric investigation of the reactions during thermal conversion of wood biomass. Biomass and Bioenergy 27, 459-465.

Theis, T.L., Singer, P.C., 1974. Complexation of iron(II) by organic matter and its effect on iron(II) oxidation. Environ. Sci. Technol. 8, 569-573.

Thompson, A., Chadwick, O.A., Boman, S., Chorover, J. 2006a. Colloid mobilization during soil iron redox oscillations. Environ. Sci. Technol. 40, 5743-5749.

Thompson, A., Chadwick, O.A., Rancourt, D.G., Chorover, J., 2006b. Iron-oxide crystallinity increases during soil redox oscillations. Geochim. Cosmochim. Acta 70, 1710-1727.

Voegelin, A., Senn, A.C., Kaegi, R., Hug, S.J., Mangold, S., 2013. Dynamic Fe-precipitate formation induced by Fe(II) oxidation in aerated phosphate-containing water. Geochim. Cosmochim. Acta 117, 216-231.

Weishaar, J.L., Aiken, G.R., Bergamaschi, B.A., Fram, M.S., Fujii, R., Mopper, K., 2003. Evaluation of specific ultraviolet absorbance as an indicator of the chemical composition and reactivity of dissolved organic carbon. Environ. Sci. Technol. 37, 4702-4708.

Wissing, L., Kölbl, A., Hausler, W., Schad, P., Cao, Z.H., Kögel-Knabner, I., 2013. Management-induced organic carbon accumulation in paddy soils: The role of organo-mineral associations. Soil Till. Res. 126, 60-71.

Wissing, L., Kölbl, A., Schad, P., Bräuer, T., Cao, Z.H., Kögel-Knabner, I., 2014. Organic carbon accumulation on soil mineral surfaces in paddy soils derived from tidal wetlands. Geoderma 228-229, 90-103.

Table 1. Chemical characteristics of the rice straw-derived DOM used in this study

Parameter	Value
C (mg g^{-1})[a]	304
N (mg g^{-1})[a]	111
H (mg g^{-1})[a]	391
O (mg g^{-1})	258
C/N	27.3
COOH acidity (mmol mol^{-1} C)[b]	23.2
Phenolic acidity (mmol mol^{-1} C)[b]	49.7
C distribution (%)[c]	
Alkyl C	22.6
Methoxy/amine C	8.3
O-Alkyl C	37
Aromatic C	19.8
Carboxyl C	6.7
Carbonyl C	5.6
Anions[d] (mmol g^{-1} C)	
Cl^-	24.1
NO_3^-	nd
SO_4^{2-}	0.1
HPO_4^-	1.2
H_4SiO_4	1.7
Cations[e] (mmol g^{-1} C)	
K^+	19.6
Ca^{2+}	4.9
Fe^{3+}	0.03

[a] Determined by dry combustion.
[b] Total and carboxyl acidity were determined by potentiometric titration with $Ba(OH)_2$ and Ca-acetate, respectively.
[c] Determined by ^{13}C-NMR spectroscopy.
[d] Determined by ion chromatography, except for Si that was determined spectrophotometrically.
[e] Determined by atomic absorption spectroscopy.

Table 2. Synthesis conditions and properties of ferrihydrite and Fe-OM associations

System	Initial solution concentrations		Molar C/Fe ratio		C content (mg g^{-1})	Fe content (mg g^{-1})	$\varepsilon/\varepsilon_0$
	C (mmol l^{-1})	Fe (mmol l^{-1})	initial solution	product[b]			
Fh	0	2.4	0.0	0.0	–	472	nd
SA1	1.9	2.1	0.9	0.1	17.8	459	0.93
SA5	11.3	2.1	5.3	1.0	39.2	447	1.06
SA10	22.2	2.1	10.5	1.0	47.4	442	1.02
CP1	1.8	2.0	0.9	0.5	49.3	411	0.14
CP5	11.1	2.0	5.6	2.7	154.6	292	0.33
CP10	21.7	2.1	10.3	4.5	213.0	243	0.67
CPf[a]	3.3 (1.7-5.0)	1.1 (0.6-2.2)	3.5 (2.0-9.5)	0.8	70.9	428	nd

[a] Values represent mean values (range) of all soil solutions collected during the cropping season.
[b] Calculated from the difference between initial and equilibrium concentrations of C and Fe in solution, except for CPf that was calculated from coprecipitate C and Fe contents.

Table 3. Specific surface area, pore characteristics and surface charge of ferrihydrite and Fe-OM associations

System	SSA (m^2 g^{-1})	Micropore volume 0.5-2 nm (mm^3 g^{-1})	Mesopore volume (mm^3 g^{-1})		Total pore volume (mm^3 g^{-1})	ζ potential (mV)
			2-10 nm	10-50 nm		
Fh	385	17	331	29	418	+28
SA1	345	15	308	37	398	–18
SA5	372	18	326	52	419	–10
SA10	291	14	265	41	339	–44
CP1	338	18	290	119	445	+29
CP5	58	4	48	38	102	–6
CP10	47	3	43	34	94	–11
CPf	171	7	16	45	106	–23

Figures

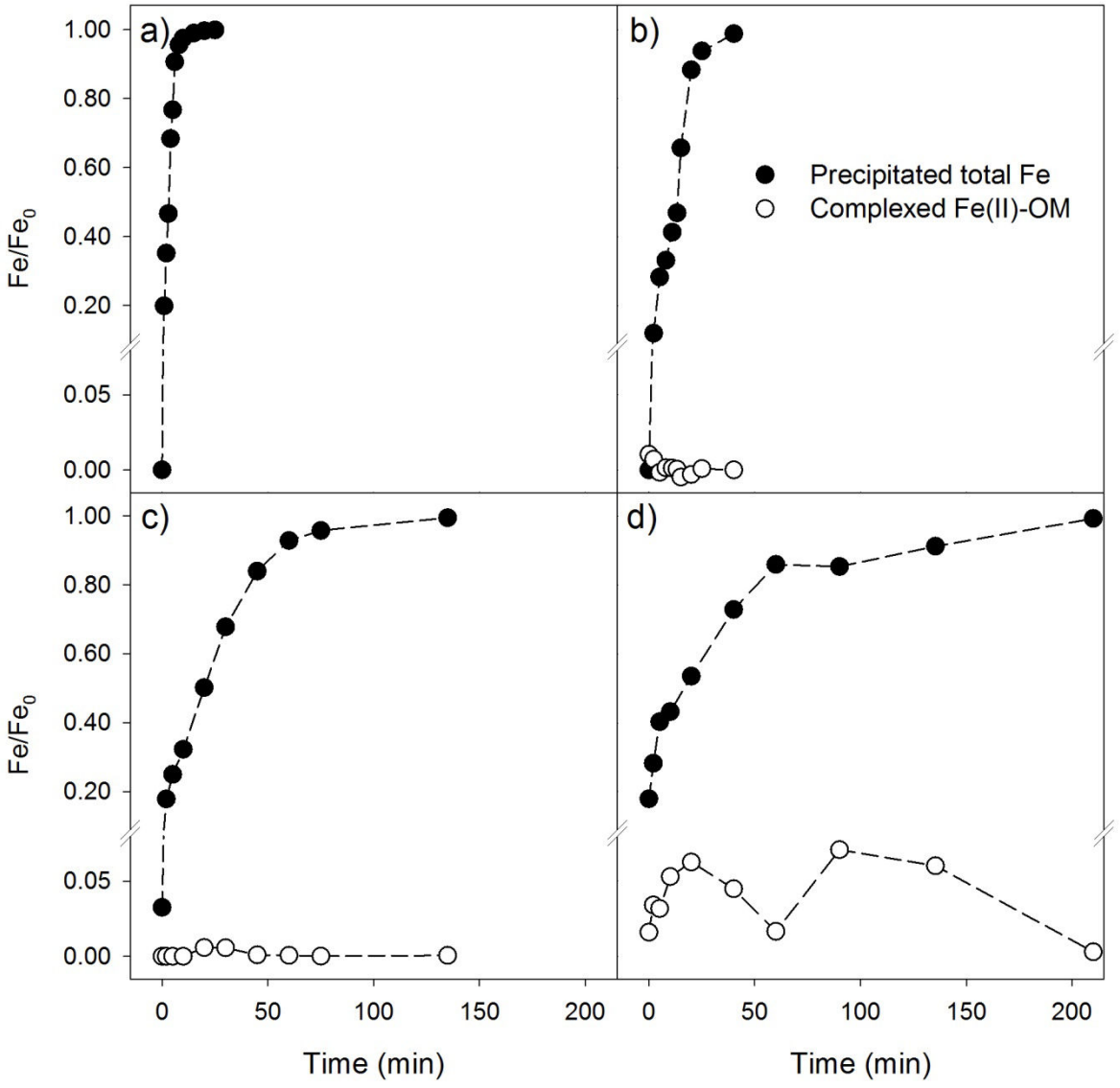

Fig. 1. Variations in the amount of precipitated total Fe (closed symbols) and organic matter complexed Fe(II) (open symbols) relative to the initial amount (Fe_0) as a function of time during the oxidative preparation of (a) Fh, (b) CP1, (c) CP5 and (d) CP10 with increasing initial molar C/Fe ratios.

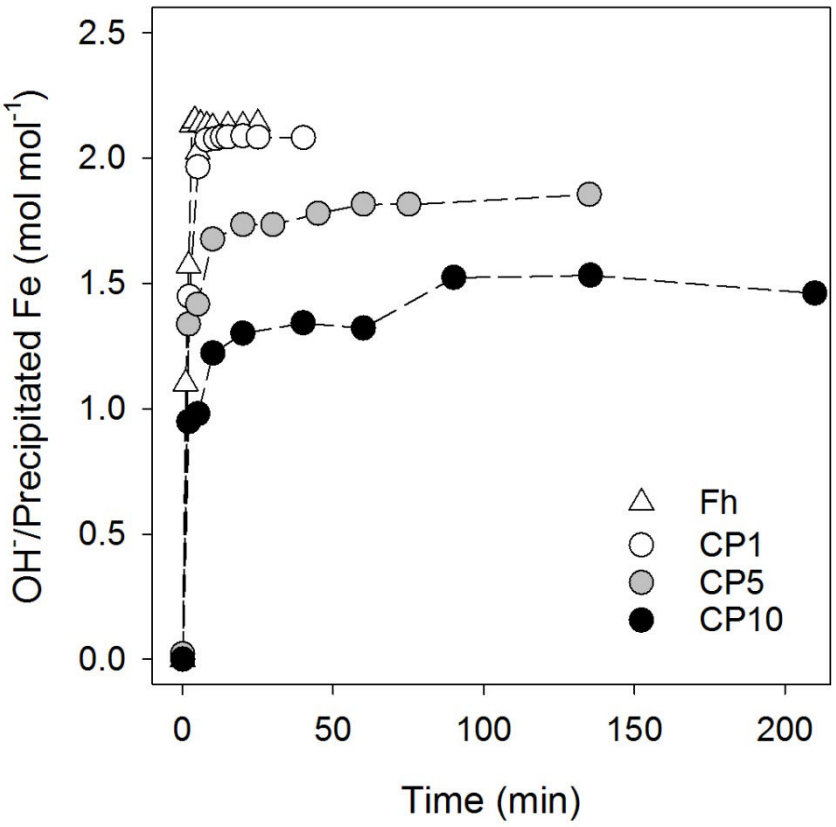

Fig. 2. Variations in the molar ratio of consumed OH^- to precipitated Fe as a function of time during the oxidative preparation of (a) Fh, (b) CP1, (c) CP5 and (d) CP10 with increasing initial molar C/Fe ratios.

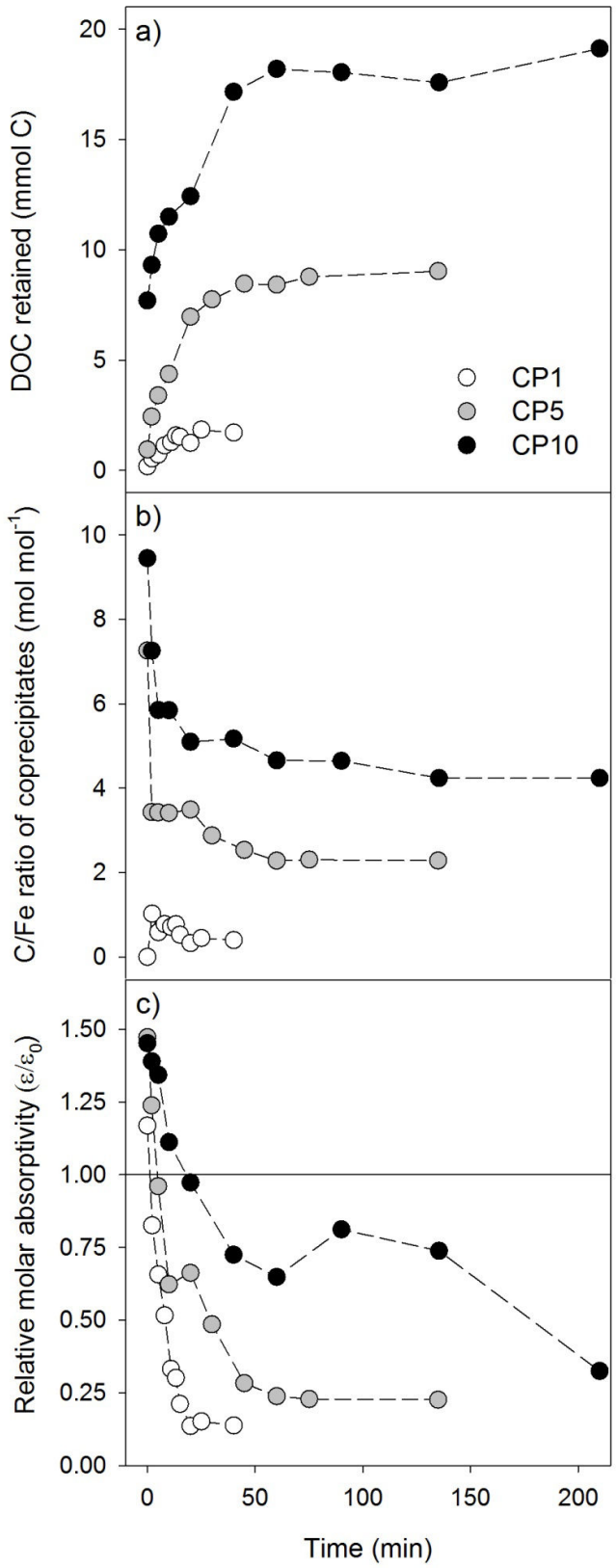

Fig. 3. Variations in (a) absolute amount of DOC retained, (b) C/Fe ratio of the coprecipitate formed, and (c) the relative molar UV absorbance at 254 nm of DOM remaining in solution, as a function of time during the preparation of Fe-OM coprecipitates with increasing initial molar C/Fe ratios.

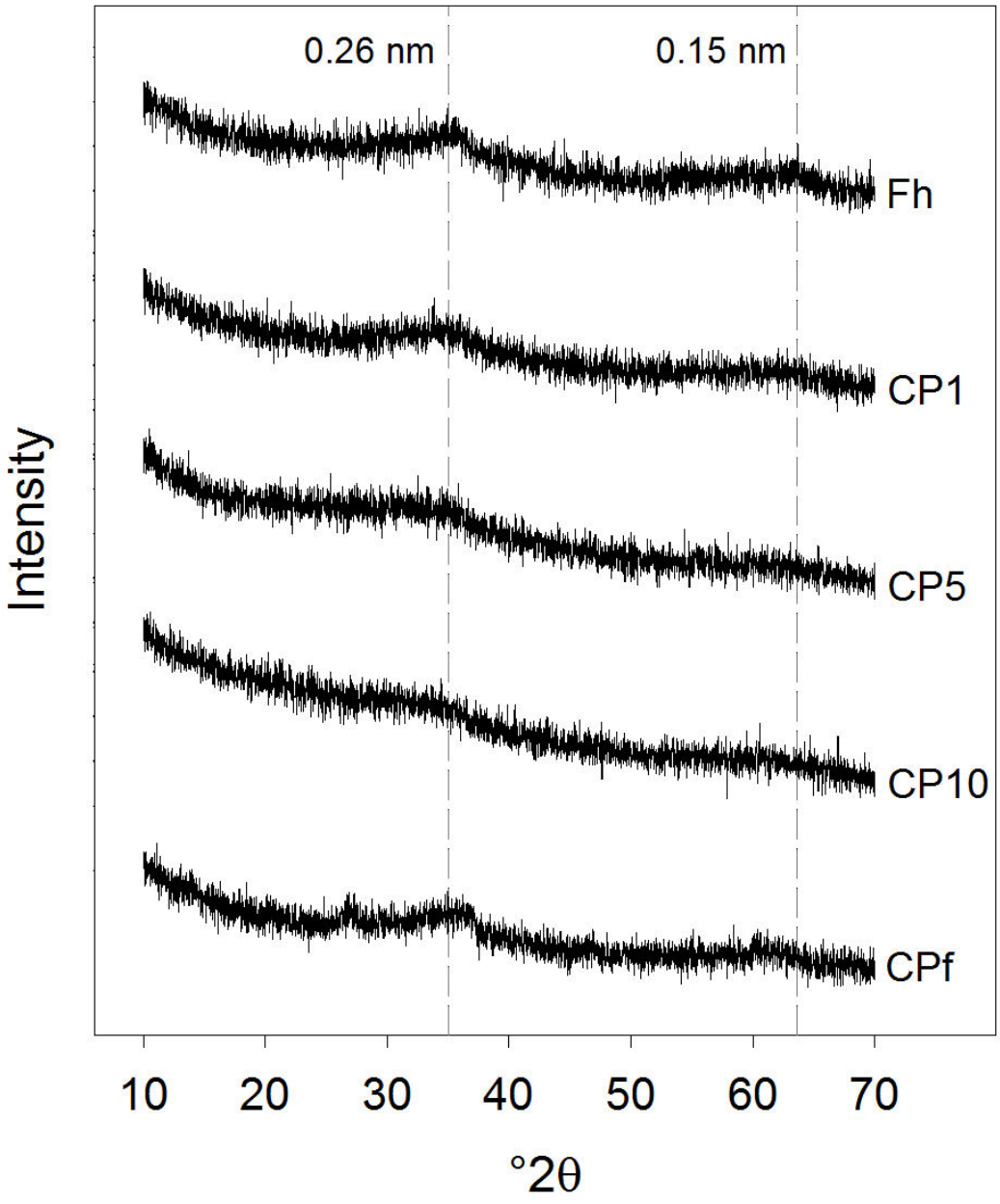

Fig. 4. X-ray diffractograms of ferrihydrite (Fh) and Fe-OM coprecipitates obtained from the oxidation and hydrolysis of Fe^{2+}. Labels represent *d*-spacing values expressed in nm.

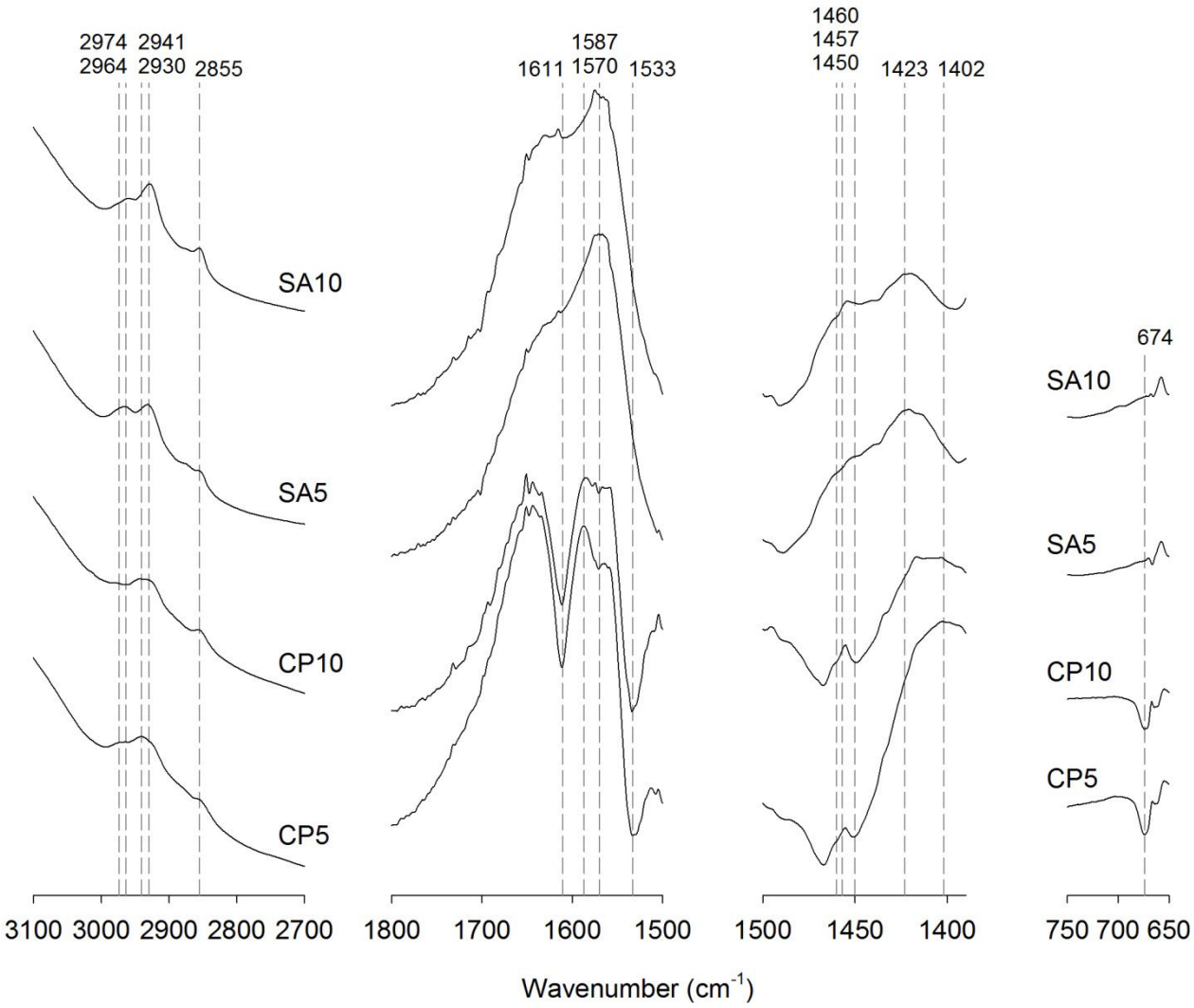

Fig. 5. FTIR difference spectra of DOM retained by surface adsorption (SA5 and SA10) and coprecipitation (CP5 and CP10).

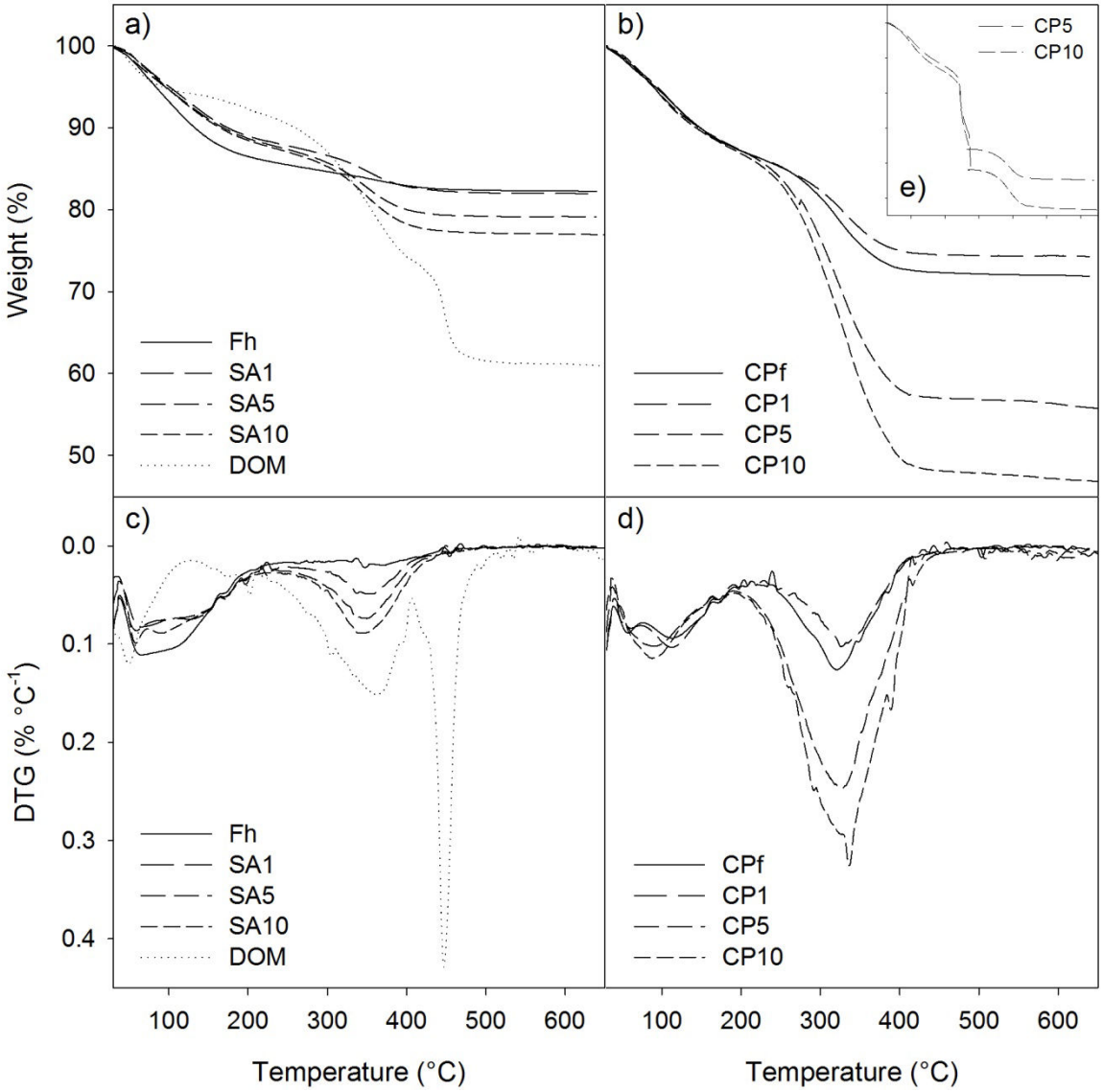

Fig. 6. Thermogravimetric mass loss (a, b, e) and differential thermogravimetric (c, d) curves of DOM, ferrihydrite (Fh) and the different surface adsorbed and coprecipitated Fe-OM associations. Inlay (e) shows TG curves obtained from the analysis of coprecipitates CP5 and CP10 when a higher aliquot mass (~15 mg) was utilized.